Enhancement of the luminous characteristics of the laminated OLEDs

DONG-HEON YOO, CHEOL-HEE MOON*
Department of Semiconductor Engineering, Hoseo University, Asan 314919, South Korea

The anode and cathode substrates were manufactured separately using solution processes and combined by a lamination. We created an adhesive layer by mixing polyethyleneimine (PEI), polyethylene glycol (PEG), and D-Sorbitol for both physical and electrical contact. To improve the luminous characteristics of the adhesive solution-processed OLEDs, we added TPBi, BCP, and PBD into the device layers. Our results revealed that OLEDs containing the PBD mixture achieved superior performance, reducing operating voltage by 3V, and significantly increasing current density to 1631 mA/cm² and luminance to 9665 cd/m², which are 5 and 3.5 times higher than devices without PBD.

1. Introduction

Organic light-emitting diodes (OLEDs) play a significant role in the fields of displays and lighting due to their excellent luminous characteristics, wide viewing angles, and high contrast ratios. The traditional vacuum deposition method for fabricating OLEDs has disadvantages, such as high costs and complex processes, limiting its application to large-scale production, thus prompting the exploration of solution processing as an alternative. While solution processing offers advantages in material use efficiency and allows large-area processing without the need for expensive equipment or complex high-vacuum steps [1], a fundamental issue arises as the solvent used for forming each layer can dissolve the previously formed layers, leading to intermixing of layers [2]. Various methods based on solution process techniques have been studied, including fabrication in ambient conditions using roll-to-roll processes [2], slit coating [3], inkjet printing [4], and spin-coating [5]. Among the various methods, the lamination technique utilises two substrates, making it a suitable approach for cost-effective, large-area OLED lighting production, with significant technological developments achieved and diverse results reported. Liu et al. used poly(9,9-dioctylfluorenyl-2,7-diyl) (PF) as the emitting layer and added potassium to PF for n-doping to form the electron transport layer, fabricating under an argon atmosphere [6]. Minami et al. deposited an aluminium-lithium alloy on both sides of a Polyethylene naphthalate (PEN) substrate to form the cathode, then laminated it with a glass substrate coated with functional layers and the anode, achieving a maximum luminance of 3200 cd/m^2 [7]. Miyagawa et al. coated a glass substrate with an anode and poly[2-methoxy-5-(2'-ethylhexyloxy)-1,4-phenylene vinylene] (MEH-PPV), formed the cathode on a polyethylene terephthalate (PET) substrate, and laminated these to produce a luminance of 2500 cd/m^2 [8]. Guo et al.

prepared the anode by coating a hole transport layer on an ITO-glass substrate and the cathode by coating the emitting and electron injection layers on a PET substrate before low-temperature laminating [9]. Chang et al. used non-alkali metal electrodes and introduced a sacrificial layer of polyethylene glycol (PEG) and polystyrene (PS) on polydimethylsiloxane (PDMS) to form the cathode layer, achieving a luminance of 3500 cd/m^2 through lamination [10].

However, several technical challenges still exist in reliably producing laminated OLEDs. Firstly, the physical properties at the interface must be improved. It is known that lower surface roughness enhances adhesion [11] and facilitates charge injection [12], necessitating consideration in this area. Additionally, the adhesion characteristics between the two substrates are crucial, for which the use of conductive adhesives containing D-Sorbitol to enhance the adhesion properties of polymeric materials [13], or the use of PEG to strengthen the physical adhesion with the aluminium layers during lamination [10], has been suggested. Secondly, for effective injection of electrons, which have lower mobility than holes in organic materials, from the cathode, it is essential to reduce the energy barrier between the metal electrode of the cathode substrate and the organic functional layers [10]. Significant research has been reported in this area. For instance, Zhou et al. found that when polyethyleneimine (PEI) is coated on metals or conductive materials, it reduces the work function of the metal interface by facilitating charge transfer from the amines in the self-assembled monolayers (SAMs) across the interface, with thinner PEI films lowering the work function more substantially [14]. Based on this research, Kim et al. treated PEDOT:PSS with PEI, reducing the work function from 5.1 eV to 3.97 eV [15], while Jenekhe's team reported that PEI treatment reduced the work function of ITO/ZnO layers by about 1 eV, with higher molecular weight of PEI extending the lifespan of

organic layers [16].

In summary, for the stable fabrication of bonded devices, the bonding layer that joins two substrates must satisfy both adhesive and electrical properties. In previous studies, we have prepared an adhesive solution by mixing PEI and PEG, applied it by spin-coating, and then laminated the cathode and anode substrates to fabricate solution-processed OLED devices [17-19], reporting a maximum luminance of 2700 cd/m^2 when 0.1 wt% PEI and 0.01 wt% PEG was mixed [19]. Considering that the luminance of vacuum-deposited monochrome OLEDs typically ranges from 10000 to 23000 cd/m^2[20], and that of solution-processed monochrome OLEDs ranges from 7000 to 15000 cd/m^2 [21,22], the luminance is significantly lower, thus this paper aims to improve the luminance characteristics. To increase luminance, it is crucial to ensure that the injected electrons effectively combine with the holes in the emitting layer. This requires enhancing the electron transport ability from the cathode to the emitting layer and preventing holes from bypassing the emitting layer. Materials used for such purposes in OLEDs include 2,2′,2″-(1,3,5-benzinetriyl)-tris(1-phenyl-1-H-benzimidazole) (TPBi) [23], 4,7-Diphenyl-1,10-phenanthroline (Bphen) [24], 2,9-Dimethyl-4,7-diphenyl-1,10-phenanthroline (BCP) [25], 2-(4-Biphenyl)-5-(4-tert-butylphenyl)-1,3,4-oxadiazole (PBD) [26,27], 3-(4-Biphenyl)-4-phenyl-5-tert-butylphenyl-1,2,4-triazole (TAZ) [28], and 8-Hydroxyquinolinolato-lithium (Liq) [29]. In this paper, we explore the use of materials such as TPBi [30], BCP [31], and PBD [32] for the electron transport layer in solution-processed OLEDs. These materials were employed either as independent layers or mixed into the emissive to enhance electron transport and block holes from passing through the emissive layer, thereby increasing electron-hole recombination efficiency.

2. Experimental

2.1. Synthesis of the material for the adhesive layer

In previous studies, the optimal conditions for the adhesive layer were achieved by using 0.05 wt% of PEI (750k, Sigma-Aldrich, Germany) as a metal surface modifier and 0.01 wt% of PEG (6k, Sigma-Aldrich, Germany) as a polymer electrolyte in ethanol. These components were stirred together and dissolved using ethanol as a solvent for 12 hours. For the comparison, an adhesive solution was also prepared by mixing 0.05 wt% of PEI and 0.05 wt% of D-sorbitol [19]. To enhance the luminous performance of laminated OLEDs through electron transport and hole blocking, solutions of TPBi, BCP, and PBD were prepared as follows: TPBi (LT-E302, Lumtec Corp., Taiwan) was mixed at a concentration of 0.5 wt% in acetone, BCP (LT-E304, Lumtec Corp., Taiwan) was also prepared at 0.5 wt% in ethanol, and PBD (LT-E303, Lumtec Corp., Taiwan) was mixed at 0.5 wt% in acetone. Each solution was stirred for 12 hours to ensure thorough mixing. For the fabrication of the emissive layer (EML), the host material PDY-132 (Super Yellow PPV, Sigma-Aldrich, Germany) was added to

chlorobenzene at a concentration of 0.5 wt% to create a solution comprised solely of the host material. Additionally, solutions doped with PBD were prepared at the same PDY-132 concentration with varying levels of PBD:0.1 wt%, 0.5 wt%, and 1.0 wt%. Each solution was stirred for 8 hours.

2.2. Fabrication of single-substrate devices

In this study, a single-layer device refers to a structure where all functional layers are formed on a single substrate, similar to the typical deposition process used in OLEDs. The purpose of fabricating single-layer devices was to determine the impact of the adhesive layer on charge transport without considering its physical adhesive function, which is one of the two primary roles of the bonding layer. Fig. 1(a) represents the basic adhesive layer structure previously reported by our research team [19], where PEDOT:PSS (Al4083, CLEVIOS, Germany) solution was spin-coated at 4000 rpm and then thermally treated at 200 °C on ITO, followed by spin-coating of PDY-132 solution at 1500 rpm and thermal treatment at 100 °C. Subsequently, an adhesive mixture of PEI and PEG was spin-coated at 2000 rpm and thermally treated at 100 °C, before cathode formation through thermal evaporation of Ag in a vacuum chamber at a rate of 5.0 Å/s to a thickness of 1.1 kÅ. To enhance the luminance of the devices, this research explored two modifications: adding materials like TPBi, BCP, and PBD as separate layers between the emissive and adhesive layers [Fig. 1(b)], and mixing them into the emissive layer [Fig. 1(c)]. These materials were applied by spin-coating at 2000 rpm and subsequently thermally treated at 100 °C.
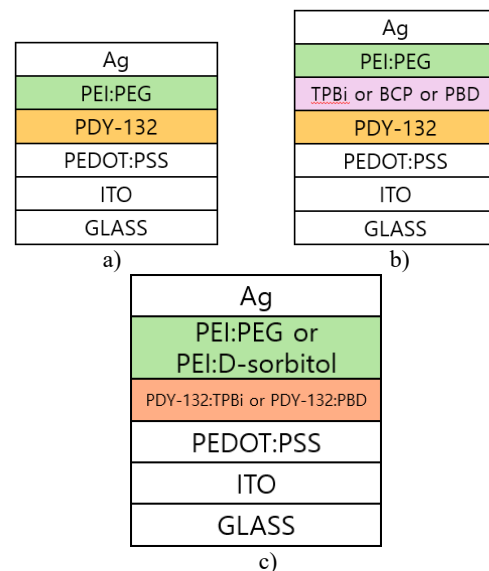

Fig. 1. Device structures of the single substrate OLEDs: (a) standard structure; (b) additives in the form of additional layer; (c) additives mixed with EML (color online)

2.3. Fabrication of laminated devices

To enhance the luminance of laminated OLED devices, based on the performance evaluation of single-layer devices, conditions expected to yield favourable characteristics were applied to fabricate laminated devices.

Fig. 2(a) employs a structure using a basic adhesive layer previously reported in our publications [19], fabricated as follows: a PEDOT:PSS solution was spin-coated at 4000 rpm on an ITO-patterned substrate and annealed at 200 °C, followed by spin-coating a light-emitting layer of PDY-132 or a mixture of PDY-132 with PBD at 1500 rpm, which was then annealed at 100 °C. On the opposite substrate, Ag was deposited on a colorless PI (CPI) film in a vacuum chamber by thermal evaporation at a rate of 5.0 Å/s to a thickness of 1.1 kÅ to form the cathode. The adhesive layer that connects the two substrates, consisting of a mixture of PEI and PEG [Fig. 2(b)] or PEI and D-sorbitol [Fig. 2(c)], was spin-coated at 2000 rpm and annealed at 100 °C. These two prepared substrates were then laminated using a roller heated to 110 °C to fabricate the laminated OLED devices.

The fabricated single-layer and laminated devices were assessed using an OLED parameter tester (M3000, McScience, Korea) to measure current density and luminance.
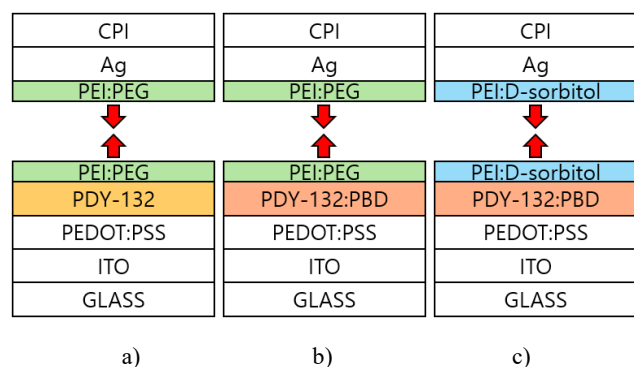

Fig. 2. Device structures of the two substrate OLEDs: (a) standard structure; (b) adhesive layer of PEI and PEG mixture and EML layer mixed with PBD; (c) adhesive layer of PEI and D-sorbitol mixture and EML layer mixed with PBD (color online)

3. Results and discussions

3.1. Single-substrate devices

Table 1 summarises the conditions of the single-layer devices fabricated in this study. A represents the baseline device, employing PDY-132 as the emitting layer and a mixture of PEI and PEG as the electron-injection layer. B, C and D are configurations where TPBi, BCP, and PBD, respectively, have been added as separate layers between the emitting and electron-injection layers of device A. Table 2 summarises the energy levels of three materials. In contrast, B[m] and D[m] represent structures where TPBi and PBD, respectively, have been added by mixing into the emitting layer, to examine how the effects differ depending on the method of incorporation into the device, even when using the same materials. However, BCP was excluded from the experiments due to poor mixing with the emitting layer. D[m,S] is a variation of the D[m] structure where PBD is mixed into the emitting layer, but the

adhesive layer has been altered by mixing PEI with D-sorbitol, to investigate how changes in the type of adhesive layer affect the outcomes of the experiment.

Table 1. Comparison of layer configurations of the single-substrate OLEDs

A	PEDOT:PSS / PDY-132		/PEI:PEG
B	PEDOT:PSS / PDY-132	/TPBi	/PEI:PEG
C	PEDOT:PSS / PDY-132	/BCP	/PEI:PEG
D	PEDOT:PSS / PDY-132	/PBD	/PEI:PEG
B[m]	PEDOT:PSS / PDY-132:TPBi		/PEI:PEG
D[m]	PEDOT:PSS / PDY-132:PBD		/PEI:PEG
D[m,S]	PEDOT:PSS / PDY-132:PBD		/PEI:D-sorbitol

Table 2. Comparison of energy level of the added substances

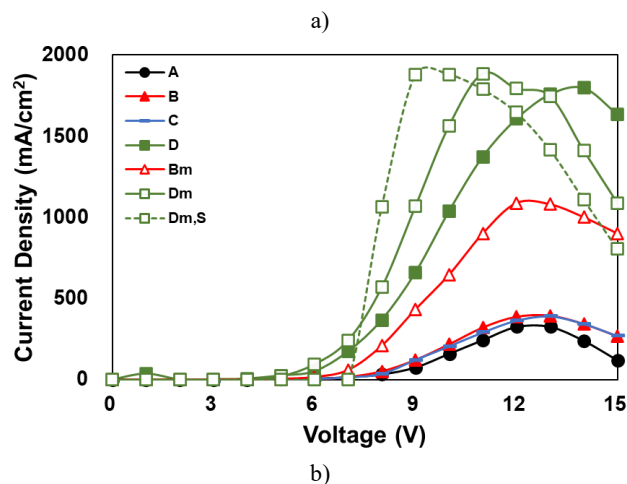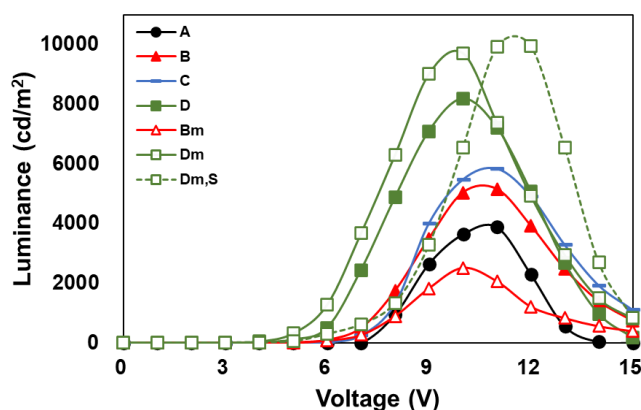|	LUMO (eV)	HOMO (eV)
TPBi	-2.7	-6.7
BCP	-3.0	-6.5
PBD	-2.5	-6.0

a)

b)

Fig. 3. Characteristics of the single-substrate OLEDs manufactured with various conditions listed in Table 1. (a) Luminance (b) Current density (color online)

Fig. 3 illustrates the characteristics of the single-layer devices fabricated under the conditions summarized in Table 1. Fig. 3(a) shows the luminance characteristics where the driving voltage of the OLED devices (at a brightness of 1 cd/m^2) reveals that the baseline device A operated at 6 V, whereas devices B, C, and D, which had additional layers of TPBi, BCP, and PBD respectively, showed reduced operating voltages of 4-5 V. Similarly, devices B^m and D^m, which incorporated TPBi and PBD into the emitting layer, exhibited reduced driving voltages of 4 V and 5 V respectively. A closer look at the luminance increase in Fig. 3(a) indicates that devices incorporating PBD generally showed higher brightness at 2-3 V lower than those mixing TPBi or BCP (B, C). Despite the work function of Ag being 4.7 eV, and TPBi, BCP, and PBD having work functions of 2.7, 3.0, and 2.5 eV respectively, one might expect the driving voltage of PBD-based devices to be higher based on work function differences alone; however, the actual results proved otherwise. Contrary to expectations, the devices with PBD added showed the lowest driving voltage, possibly due to the oxadiazole units in PBD increasing the electron affinity in the emitting and polymer layers, allowing the device to operate at lower voltages [33]. Examining the voltage dependent luminance characteristics in Fig. 3(a), the baseline device A showed a brightness of 3875 cd/m^2, while devices B, C, and D with additional layers of TPBi, BCP, and PBD showed brightness levels of 5147, 5826, and 8178 cd/m^2 respectively. The maximum luminance measured for devices B^m and D^m, which had TPBi and PBD mixed into the emitting layer, were 2503 cd/m^2 and 9713 cd/m^2 respectively. PBD showed the highest luminance, which can be attributed to the lowered energy barriers by the oxadiazole units in PBD, leading to an increased injection of electrons into the emitting layer, and the high HOMO energy levels of PBD preventing easy transition of holes to the electron layer, thereby enhancing recombination of electrons and holes within the emitting layer. Fig. 3(b) shows the current density where the baseline device A exhibited a maximum current density of 326 mA/cm^2 at 13 V, whereas devices B, C, and D, with additional layers of TPBi, BCP, and PBD, showed current densities of 393, 390, and 1798 mA/cm^2, respectively.

Notably, devices with PBD demonstrated more than a five-fold increase in current density compared to other conditions. Devices B^m and D^m, which incorporated TPBi and PBD into the emitting layer, exhibited maximum current densities of 1088 and 1886 mA/cm^2, respectively. Overall, the inclusion of PBD not only showed a significant increase in current density compared to TPBi and BCP but also resulted in high luminance values for both methods of insertion (as a separate layer in D and mixed into the emitting layer in D^m), with the latter achieving the maximum current density at about 3 V lower. For the optimal condition D^m, modifying the adhesive layer composition in D^{m,S} by mixing PEI with D-sorbitol showed similar maximum current densities but at about 2 V lower voltage.

The conclusion drawn from Fig. 3(a) and 3(b) is that PBD, regardless of its integration method (either as a separate layer or mixed into the emissive layer) or the type of adhesive layer used (mixed with PEI and PEG or D-sorbitol), consistently enhances both luminance and current density across all scenarios. This effect can be attributed to the high electron affinity of PBD's oxadiazole units, which enhance electron transport capabilities by increasing the electron affinity within the emissive layer or polymer materials [33]. Fig. 4 illustrates the recombination process in OLED devices where holes injected from the anode and electrons from the cathode meet in the emissive layer, PDY-132. To achieve high luminance, both electrons and holes need to be abundant in the emissive layer. The initial electron injection from the Ag electrode to the PEI:PEG layer is determined by the work function difference between these materials. Subsequently, the quantity of electrons transitioning to the next layer is governed by the mobility within the PEI:PEG layer, which decreases with increased layer thickness. The mobility changes once more in the electron transport layer, PBD, ultimately defining the quantity of electrons transitioning into the emissive layer. According to the results in Fig. 3, the integration of PBD, whether as a separate layer or mixed into the emissive layer, leads to an increase in luminance, explained by the enhanced electron affinity of PBD improving electron mobility during the transition from the PEI:PEG layer to the PDY-132 layer.
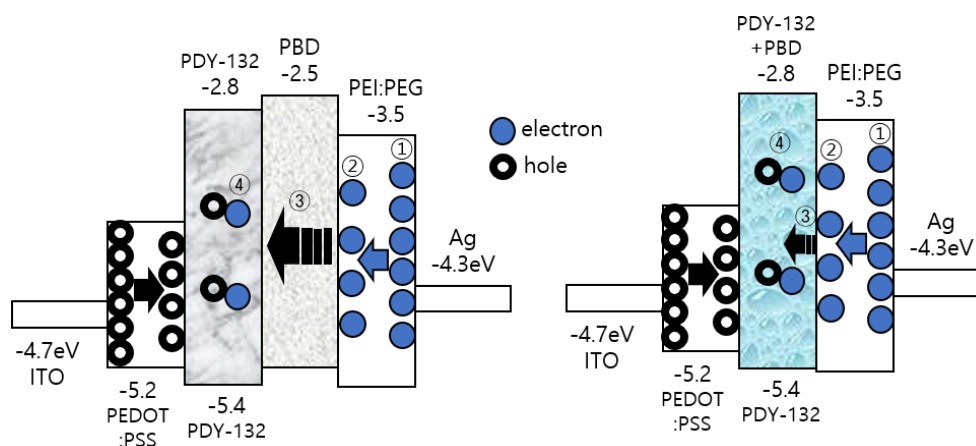

Fig. 4. Energy diagram for the OLED device with PBD; (a) as an additional layer (b) as mixed with EML (color online)

3.2. Laminated devices

Table 3 summarises the conditions of the adhesive devices fabricated in this study, with (L) denoting devices made using the lamination method. From the results of single-substrate devices evaluated in Fig. 3, the D^m structure (PDY-132 mixed with PBD) exhibited the best properties and was thus chosen for the fabrication and evaluation of the laminated OLEDs. This involved comparing the basic A condition (without PBD) and D^m and also fabricating devices with an adhesive layer mixed with PEI and D-sorbitol to assess changes in properties due to adhesion.

Table 3. Comparison of layer configurations of the double-substrate, laminated OLEDs

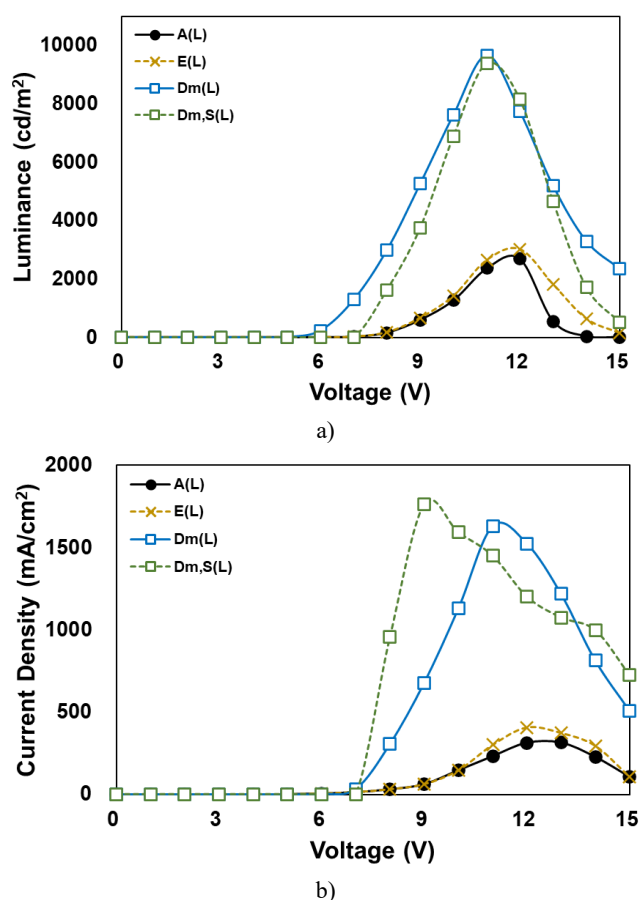|		
A(L)	PEDOT:PSS / PDY-132	/ PEI:PEG
E(L)	PEDOT:PSS / PDY-132	/ PEI:D-sorbitol
D^m(L)	PEDOT:PSS / PDY-132:PBD	/ PEI:PEG
$D^{m,S}$(L)	PEDOT:PSS / PDY-132:PBD	/ PEI:D-sorbitol

a)

b)

Fig. 5. Characteristics of the double-substrate, laminated OLEDs manufactured with various conditions listed in Table 3. (a) Luminance (b) Current density (color online)

Fig. 5(a) illustrates the luminance characteristics of OLED devices in terms of operating voltage (voltage at 1 cd/m² luminance). For the basic device, A(L), the operating voltage is 7 V, whereas for the D^m(L) device, which incorporates PBD into the emissive layer, the voltage drops to 4-5 V. Moreover, the maximum luminance of the D^m(L) device reaches 9665 cd/m², more than 3.5 times higher than the 2700 cd/m² of the A(L) device. This luminance is similar to the 9713 cd/m² observed in the D^m device from Fig. 3, indicating comparable luminance characteristics between the planar and adhesive devices. For devices with an adhesive layer made from a mix of PEI and D-sorbitol, the luminance does not vary significantly whether PBD is included or not, as shown by the E(L) device's maximum luminance of 3020 cd/m² and the $D^{m,S}$(L) device's 9400 cd/m², suggesting that the choice of mixing PEI with either PEG or D-sorbitol does not substantially affect luminance.

Fig. 5(b) illustrates the current density characteristics, where the A(L) device exhibited a current density of 314 mA/cm² at 13 V, while the D^m(L) device showed a significantly enhanced current transportation of 1631 mA/cm² at 11V, approximately five times higher at 2 V lower voltage. For devices with an adhesive layer mixed with D-sorbitol, the base E(L) device showed a current density of 407 mA/cm², and the $D^{m,s}$(L) device, which incorporated PBD into the emissive layer, exhibited 1593 mA/cm², indicating no difference from devices where the adhesive layer was mixed with PEG.

Summarising the results, we can conclude as follows. Firstly, the introduction of PBD as an electron transport layer not only enhanced the luminance and current density in the single-layer devices shown in Fig. 3 but also in the adhesive devices in Fig. 5, indicating that the oxadiazole doping effect of PBD is effective in adhesive devices as well. Secondly, in the case of adhesive devices, the adhesive layer provides not only physical adhesion but also influences electron mobility; the combination of PEI with either PEG or D-sorbitol satisfies both characteristics of the adhesive layer. Here, the roles of PEG or D-sorbitol can be described as compensating for the inadequate adhesive strength of PEI. During this time, the use of PEG, with its low melting point of 60 °C, has been found to cause issues such as uniformity during the lamination process, whereas D-sorbitol, with a relatively higher melting point of 95 °C, allows for appropriate usage of these materials depending on their application in the lamination process.

4. Conclusion

To achieve both a physical and an electrical contact in a two-substrates, laminating process, an adhesive layer was created by mixing polyethylenimine (PEI), polyethylene glycol (PEG), and D-Sorbitol. To enhance the luminous characteristics of the devices, we added TPBi, BCP, and PBD into the layers of the device. The results showed that PBD consistently and most

effectively enhances both luminance and current density. It is explained that the oxadiazole doping effect of PBD is effective in adhesive devices, providing not only physical adhesion but also electron mobility. The combination of PEI with either PEG or D-sorbitol satisfies both characteristics of the adhesive layer. The adhesive OLEDs with PBD mixture exhibited the best performance, 3V reduction in operating voltage, and the current density and luminance were enhanced to 1631 mA/cm² and 9665 cd/m², respectively 5 and 3.5 times higher than those without addition.

Acknowledgements

References

[1] K. S. Yook, J. Y. Lee, Advanced Materials **26**(25), 4218 (2014).

[2] N. Aizawa, Y. J. Pu, M. Watanabe, T. Chiba, K. Ideta, N. Toyota, M. Igarashi, Y. Suzuri, H. Sasabe, J. Kido, Nature Communications **5**(1), 5756 (2014).

[3] H. Youn, K. Jeon, S. Shin, M. Yang, Organic Electronics **13**(8), 1470 (2012).

[4] C. Kant, A. Shukla, S. K. McGregor, S. C. Lo, E. B. Namdas, M. Katiyar, Nature Communications **14**(1), 7220 (2023).

[5] H. Zheng, Y. Zheng, N. Liu, N. Ai, Q. Wang, S. Wu, J. Zhou, D. Hu, S. Yu, S. Han, Nature Communications **4**(1), 1971 (2013).

[6] J. Liu, L. N. Lewis, T. J. Faircloth, A. R. Duggal, Applied Physics Letters **88**(22), 223509 (2006).

[7] T. Minani, R. I. Satoh, H. Okada, S. Naka, Japanese Journal of Applied Physics **50**(1S2), 01BC12 (2011).

[8] M. Miyagawa, R. Koike, M. Takahashi, H. Bessho, S. Hibino, I. Tsuchiya, M. Harano, M. Endo, Y. Taniguchi, Japanese Journal of Applied Physics **46**(11R), 7483 (2007).

[9] T. F. Guo, S. Pyo, S. C. Chang, Y. Yang, Advanced Functional Materials **11**(5), 339 (2001).

[10] Y. F. Chang, C. Y. Chen, F. T. Luo, Y. C. Chao, H. F. Meng, H. W. Zan, H. W. Lin, S. F. Horng, T. C. Chao, H. C. Yeh, Organic Electronics **13**(3), 388 (2012).

[11] T. Tong, B. Babatope, S. Admassie, J. Meng, O. Akwogu, W. Akande, W. O. Soboyejo, Journal of Applied Physics **106**(8), 083708 (2009).

[12] T. F. Guo, G. He, S. Pyo, Y. Yang, Applied Physics Letters **80**(21), 4042 (2002).

[13] J. Ouyang, Y. Yang, Advanced Materials **18**(16), 2141 (2006).

[14] Y. Zhou, C. Fuentes-Hernandez, J. Shim, J. Meyer, A. J. Giordano, H. Li, P. Winget, T. Papadopoulos, H. Cheun, J. Kim, Science **336**(6079), 327 (2012).

[15] K. M. Kim, S. Ahn, W. Jang, S. Park, O. O. Park, D. H. Wang, Solar Energy Materials and Solar Cells **176**, 435 (2018).

[16] B. A. E. Courtright, S. A. Jenekhe, ACS Applied Materials & Interfaces **7**(47), 26167 (2015).

[17] C. H. Moon, Korean Journal of Metals and Materials **61**(3), 175 (2023).

[18] C. H. Moon, Journal of Adhesion and Interface **24**(3), 86 (2023).

[19] D. H. Yoo, C. H. Moon, Electronics **13**(1), 128 (2023).

[20] G. Liu, Z. Li, X. Hu, Y. Qin, C. S. Lee, D. Chen, L. Wang, J. Liu, P. Wang, Y. J. Pu, Nature Photonics **16**(12), 876 (2022).

[21] Y. Murat, K. Petersons, D. Lanka, L. Lindvold, L. Yde, J. Stensborg, M. Gerken, Materials Advances **1**(8), 2755 (2020).

[22] C. Y. Lin, N. W. Hu, H. W. Chang, C. Y. Lu, C. Y. Chen, C. C. Wu, Organic Electronics **28**, 25 (2016).

[23] L. Cheng, L. Hung, X. Ding, Z. Gao, C. Lee, S. Lee, Displays **21**(2-3), 51 (2000).

[24] T. Zhou, Z. Ling, Z. Tang, S. Wang, K. Guo, G. Chen, Z. Cheng, X. Dai, H. Gao, T. Xu, Physica Status Solidi (a) **215**, 14 (2018).

[25] D. X. Yuan, X. D. Yuan, Q. Y. Xu, M. F. Xu, X. B. Shi, Z. K. Wang, L. S. Liao, Physical Chemistry Chemical Physics **17**(40), 26653 (2015).

[26] E. Witkowska, I. Glowacki, T. H. Ke, P. Malinowski, P. Heremans, Polymers **14**(16), 3363 (2022).

[27] C. Yap, M. Yahaya, M. Salleh, Current Applied Physics **8**(5), 637 (2008).

[28] T. Y. Cheng, J. H. Lee, C. H. Chen, P. H. Chen, P. S. Wang, C. E. Lin, B. Y. Lin, Y. H. Lan, Y. H. Hsieh, J. J. Huang, Scientific Reports **9**(1), 3654 (2019).

[29] D. P. K. Tsang, T. Matsushima, C. Adachi, Scientific Reports **6**(1), 22463 (2016).

[30] Z. Y. Liu, S. R. Tseng, Y. C. Chao, C. Y. Chen, H. F. Meng, S. F. Horng, Y. H. Wu, S. H. Chen, Synthetic Metals **161**(5-6), 426 (2011).

[31] T. Earmme, S. A. Jenekhe, Journal of Materials Chemistry **22**(11), 4660 (2012).

[32] L. Duan, L. Hou, T. W. Lee, J. Qiao, D. Zhang, G. Dong, L. Wang, Y. Qiu, Journal of Materials Chemistry **20**(31), 6392 (2010).

[33] J. W. Jang, C. E. Lee, D. Lee, J. I. Jin, Solid State Communications **130**(3-4), 265 (2004).

*Corresponding author: chmoon@hoseo.edu